Proposal for Modeling of FWM Efficiency of QD-SOA Based on the Pump/Probe Measurement Technique

Farideh Hakimian[1], Mohammad Reza Shayesteh [*,1], Mohammad Reza Moslemi[2]

[1] Department of Electrical Engineering, Yazd branch, Islamic Azad University, Yazd, Iran

[2] Department of Electrical Engineering, Zarghan Branch, Islamic Azad University, Zarghan, Iran

Abstract: In this paper, we propose a numerical model for Four-Wave Mixing (FWM) efficiency in quantum dot semiconductor optical amplifiers (QD-SOAs). Despite the complexities of the equations governing the QD-SOAs, simple models with short computational time are essential to analyze and design them. We present equations of the QD-SOAs coherently and calculate FWM efficiency in the QD-SOA using the pump/probe technique. In this model, the rate equations take into account the occupation probabilities of each level instead of the carrier of densities. Moreover, the transfer matrix based on the pump/probe measurement technique is solved in two dimensions, space and time, using the Slice technique. The described model is implemented in the MATLAB environment. The proposed model is simpler than similar models and has a shorter computational time than them.

1. INTRODUCTION

Nonlinear effects play a major role in optical fibers and are occurred due to the changes in the refractive index of the optical medium with respect to the intensity of light propagation [1]. FWM is a nonlinear effect resulting from interactions among the optical signals in an optical material like a semiconductor. The beating of two signals (pump and probe) with different

---

* Corresponding author. Email: **shayesteh@iauyazd.ac.ir**

frequency and intensity creates a new signal that is modulated signal. It is named the conjugate signal that is less intense in comparison with the probe signal. Today, FWM specifically is used for all-optical spectral conversion in optical data communication schemes allowing for very high data rates [2]. On the other hand, SOAs are important components for optical communication systems with applications as in-line amplifiers and as practical devices in developing optical networks [3]. In addition to their linear applications, the nonlinear properties of SOA can represent it [3].

The main processes are spectral-hole burning (SHB), carrier density pulsation (CDP), and carrier heating (CH) in FWM. The analytical framework of these main processes is now widely reviewed [2]. Due to the unique properties of QDs, FWM in QD-SOAs is an attractive device in FWM applications. FWM in QD-SOA is chiefly detailed in several papers [4-7]. In addition, the advantage of QD-SOAs in comparison bulk-SOAs in FWM has two aspects: first, low conversion at long wavelengths, which are increased with QDs, and second, the asymmetric conversion, which is overcome with detuning independence using QDs [8]. InAs / InGaAs based QD-SOAs devices can provide a suitable nonlinear environment for high-efficiency FWM over telecommunications.

For the effective utilization of FWM in optical data communications, numerical modeling in various devices such as QD-SOA is essential to predict the FWM efficiency correctly. Although there are experimental and numerical published models for FWM, few articles have been reported on QD-SOA modeling of FWM efficiency [2] and [9-10]. The reported models are implemented by two sets of equations consisting of rate equations and wave propagation equations based on QDs density. By applying a delay equation approach, these models elaborate on the wave propagation equation for three signals (pump, probe, and conjugate). The numerical solution of these models is too complex and troublesome due to solve wave propagation and rate equations simultaneously. Besides, attaining convergence is challenging, and these models require a large amount of memory and long runtime [7-13]. However, it is superior to produce a simple and accurate model that can describe the nonlinear characteristics of QD-SOAs like FWM. Consequently, it can use for applications with short runtime such as Computer-Aided Design (CAD).

This paper has attempted to extinction FWM characteristics of QD-SOA by presenting coherent equations. This model consists of carrier rate equations based on the probability of occupation of energy levels in the Conduction Band (CB) and Valance Band (VB) of the QD active layer. By applying a pump/probe measurement technique, the transfer matrix is solved to measure the dynamics of nonlinear changes of refractive index and gain in SOA devices. It means the effect of changes in the amplitude and phase of the probe

signal is taken into account the pump. Consequently, changes in the gain and refractive index of the material are calculated as a function of time after beating. We solve the equations using the SLICE Technique. To the best of our knowledge, no paper is reported to calculate the FWM efficiency of QD-SOA using the SLICE Technique and the transfer matrix. In this technique, the length of the QD-SOA is broken into smaller sections and each section is considered as a smaller QD-SOA by applying the time dimension. Then, we numerically solve the rate equations and transfer matrix using the introduced algorithm and calculate the FWM efficiency.

The structure of this paper is as follows: In the second section, the structure of the investigated QD-SOA is illustrated. In the third section, the governing equations of QD-SOA are presented for nonlinear modeling. In the fourth section, the introduced model and numerical algorithms for nonlinear modeling are used to calculate the efficiency of FWM. Finally, Section 5 covers the simulation results obtained for FWM efficiency in QD-SOA.

2. THE INVESTIGATED STRUCTURE OF QD-SOA

The used structure of QD-SOA is similar to the structure described in [14]. As shown in Fig. 1, the device is an InAs / GaAs heterogeneous structure operating at a 1.3 μm and consists of an n-type GaAs substrate, the active region of the InAs / GaAs quantum dot on the two-dimensional Wetting Layer (WL) which only acts as a reservoir at the band edge.
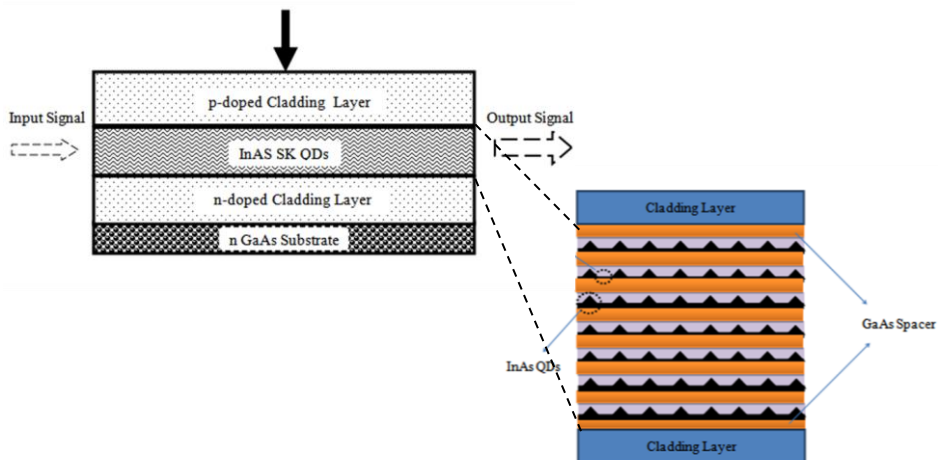
Fig. 1. The investigated structure of QD-SOA.

For the investigated structure of QD-SOA, the number of energy levels in the CB and VB are 3 and 10, respectively. The separation energy between the states in the CB and VB is also 60 and 30 meV, respectively. Also, the inhomogeneous broadening effect is 30 meV. The detailed band structure of this QD-SOA is shown in Fig. 2.
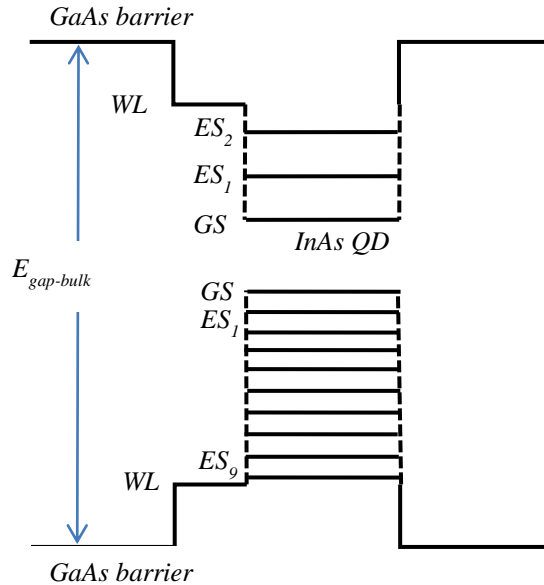
Fig. 2. The energy band diagram in the investigated QD-SOA [15].

3. REQUIRED EQUATIONS FOR NONLINEAR MODELING

A. *Rate Equations*

Rate equations are first-order ODEs that describe the dynamics of the carrier to determine the dynamics of QD-SOA. These equations for WL and Ground State (GS) and *i*-th Excited State (ES) based on occupation probability are respectively [15]:

$$\frac{df_w^k}{dt} = \frac{I}{eD_w N^{QD}} - \frac{f_w^k(1-f_M^k)}{\tau_{wM}^k} + \frac{(1-f_w^k)f_M^k}{\tau_{Mw}^k} - \frac{f_w^k}{\tau_{wR}^k} \tag{1}$$

$$\frac{df_i^k}{dt} = \frac{f_{i+1}^k(1-f_i^k)}{\tau_{i+1,i}^k} + \frac{(1-f_{i+1}^k)f_i^k}{\tau_{i,i+1}^k} \tag{2}$$

$$+ \frac{(1-f_{i-1}^k)f_i^k}{\tau_{i,i-1}^k} + \frac{f_{i-1}^k(1-f_i^k)}{\tau_{i-1,i}^k} - \frac{f_i^k}{\tau_{iR}^k}$$

$$\frac{df_0^k}{dt} = \frac{(1-f_0^k)f_1^k}{\tau_{10}^k} - \frac{f_0^k(1-f_0^k)}{\tau_{01}^k} - \frac{f_0^n f_0^p}{\tau_{0R}^k} + a_0(f_0^n + f_0^p - 1)S_{ph} \tag{3}$$

Where $i(i = 0, 1, \dots M_k)$ assigns an integer to each of the levels. If $k = n$, it indicates the quantity dependence on the electrons in the CB, and if $k = p$, it indicates the quantity depends on the holes in the VB. The definition of other quantities from (1) to (3) is given in Table I.

As an example, for the InAs / GaAs quantum dot, $M_n = 3$ and $M_p = 10$ [14]. It means that we consider 4 equations for the electron and 11 equations for the hole. The photon density is calculated from the power of input signal, which is:

$$S_{ph} = |A|^2 \tag{4}$$

Where A is the optical propagating signal, that is:

$$A = \sqrt{P}e^{i\varphi} = \sqrt{P}.(\cos\varphi + i.\sin\varphi) \tag{5}$$

Where P and φ is the power (amplitude) and phase of propagating signal in the waveguide, respectively.

TABLE I

DEFINITION OF THE PHYSICAL QUANTITIES FROM (1) TO (3) [11].

Symbol	Quantity
f_w^k	WL occupation probability by carriers
f_i^k	i-th state occupation probability by carriers
f_1^k	1-th state occupation probability by carriers
f_0^k	GS occupation probability by carriers
I	Applied current
N^{QD}	Number of Total QDs
a_0	Differential gain
τ_{0R}^k	spontaneous emission lifetime(GS)
τ_{wM}^k	Carrier Relaxation life time from WL to M-th ES
τ_{Mw}^k	Carrier escape lifetime from M-th Es to WL
τ_{wR}^k	Carrier spontaneous emission lifetime in WL
$\tau_{i+1,i}^k$	Relaxation lifetime from $(i+1)$-th to i-th state
$\tau_{i,i+1}^k$	Relaxation lifetime from i-th to $(i+1)$-th state

$\tau_{iR}{}^{k}$	spontaneous emission lifetime from i-th state
$\tau_{01}{}^{k}$	Carrier escape lifetime from Gs to first Es
$\tau_{10}{}^{k}$	Carrier relaxation lifetime from first Es to GS

B. Pump/ Probe Measurement Technique

The pump/probe measurement technique is used to measure the dynamics of nonlinear changes of refractive index and gain in SOA devices. In the basic form of this technique, there are two optical beams, one beam as a pump and the other as a weak probe. The pump is injected into the input of the amplifier to produce changes of the carrier population in the test material and probe samples changes in amplitude and phase.

In this technique, the forward and backward waves for the pump and probe signal by applying the transfer matrix is [16]:

$$\begin{bmatrix} F_{\varepsilon+1}^{j} \\ B_{\varepsilon+1}^{j} \end{bmatrix} = M_{\varepsilon}^{j} \begin{bmatrix} F_{\varepsilon}^{j} \\ B_{\varepsilon}^{j} \end{bmatrix} \tag{6}$$

Where $j = pump$ corresponds to the pump signal, $j = probe$ to the probe signal, and $j = conj$ to the conjugate signal. By breaking the length of the amplifier into the UBL sections, each section is named $\varepsilon = 1,2,...,UBL$. The matrix M_{ε}^{j} is [16]:

$$M_{\varepsilon}^{j} = \frac{1}{1-r_{j\varepsilon}^{2}} \begin{bmatrix} e^{i\gamma_{j\varepsilon}L} - r_{j\varepsilon}^{2} e^{-i\gamma_{j\varepsilon}L} & -r_{j\varepsilon}(e^{i\gamma_{j\varepsilon}L} - e^{-i\gamma_{j\varepsilon}L}) \\ r_{j\varepsilon}(e^{i\gamma_{j\varepsilon}L} - e^{-i\gamma_{j\varepsilon}L}) & e^{-i\gamma_{j\varepsilon}L} - r_{j\varepsilon}^{2} e^{i\gamma_{j\varepsilon}L} \end{bmatrix} \tag{7}$$

$$\gamma_{j\varepsilon} = \sqrt{\left(\Delta\beta_{\varepsilon}^{j}\right)^{2} - \kappa^{2}} \tag{8}$$

$$r_{j\varepsilon} = \frac{-\kappa}{\gamma_{j\varepsilon} + \Delta\beta_{\varepsilon}^{j}} \tag{9}$$

$$\Delta\beta_{\varepsilon}^{j} = \delta_{j} - i\frac{g_{\varepsilon}^{j}}{2}(1 - i\alpha_{H}) + i\frac{\alpha_{l}}{2} \tag{10}$$

Active region gain also is:

$$g = \sum_{k=0}^{q} g_{densk}.(f_{k}^{n} + f_{k}^{p} - 1) = \tag{11}$$

$$g_{dens0}.(f_{0}^{n} + f_{0}^{p} - 1) + g_{dens1}.(f_{1}^{n} + f_{1}^{p} - 1) + ..$$

Where q is the number of transitions (in this model we have 3 transitions), and g_{densk} is the gain of photon energy between two identical states in both bands, and is defined as a Gaussian function, as follow [11]:

$$\Delta\beta_{\varepsilon}^{j} = \delta_{j} - i\frac{g_{\varepsilon}^{j}}{2}(1 - i\alpha_{H}) + i\frac{\alpha_{l}}{2} \tag{12}$$

The definition of other quantities from (7) to (12) is given in Table II.

C. Equations for FWM Efficiency

The effect of FWM on QD-SOA is investigated when the pump signals (A_{pump}) and probe (A_{probe}) are injected into the input facet of the amplifier. In this case, the beating between the pump and the probe modulates the carrier density and produces the conjugate signal (A_{conj}). The beating between the pump and the probe signals induces a change in the occupation probability of the levels [10].

For the aim of calculating FWM, it is necessary to calculate the photon density of each signal, as follow [16]:

$$S_{ph}^{j} = \left|F^{j}\right|^{2} + \left|B^{j}\right|^{2} \tag{13}$$

Finally, the total density of the photon is [10]:

$$S_{ph-total} = S_{ph}^{pump} + S_{ph}^{probe} + S_{ph}^{conj} \tag{14}$$

The FWM efficiency is [17]:

$$\eta = \frac{\left|F^{conj}(t, z = L)\right|^{2}}{\left|F^{probe}(t, z = 0)\right|^{2}} \tag{15}$$

TABLE II
DEFINITION OF THE PHYSICAL QUANTITIES FROM (7) TO (12) .

Symbol	Quantity
κ	Coupling coefficient
δ_j	Initial detuning
α_l	Waveguide loss
g_k^{max}	Maximum gain Coefficient for k-th transition
σ	Inhomogeneous broadening
$\varDelta\beta^j$	Detuning of wave number from Bragg wave number
α_H	Linewidth enhancement factor
G	Active region gain
$\hbar\omega_k^{max}$	Photon Energy emitted from k-th Transition of QDs
$\hbar\omega$	Input Signal Photon Energy

4. NUMERICAL MODELING FOR QD-SOA

In this modeling, from (1) to (3) must be numerically solved to model carrier dynamics. So, fifteen highly-coupled ODEs are extracted according to the number of energy levels, which are solved by the fourth-order Runge Kutta method.

On the other hand, it is essential to solving the wave propagating equation by the pump/probe measurement technique synchronously. Thus, the (6) is solved for the pump, probe, and conjugate signals, and then forward and backward signals of all three waves in the new dimension are calculated. By applying (13) and (14), the photon density is obtained. Solving (6), which involves both spatial and temporal dimensions, is very complex. Therefore, a new algorithm is required to solve these coupled equations numerically, as shown in Fig. 3.

In this way, we need to define the initial conditions for the signals as follows [10] and [11]:

$$F^{conj}(0,t) = 0 \tag{16}$$

$$F^{pump}(0,t) = \sqrt{0.1A(0,t)} \tag{17}$$

$$F^{probe}(0,t) = \sqrt{0.01A(0,t)} \tag{18}$$

$$A(0,t) = P_s . \exp(-\frac{2.t^2}{\delta_p^2}) \tag{19}$$

Where P_s is the maximum input value, and δ_p is the width of the input signal. To P_s simplify [16]:

$$P_s = \frac{N_D}{g_0^{max} . \tau_{0R}} \tag{20}$$

Where N_D is the volume density of the QDs.

In this algorithm, relying on the SLICE Technique method (Fig. 4) and applying pump and probe equations, equations (6) to (14), occupation probabilities of each level, active region gain, optical signal amplitude and photon density for next section of QD-SOA are estimated for pump, probe and conjugate signals. As shown in Fig. 4, the length of the amplifier is divided into equal parts.

Applying the initial conditions for the occupation probabilities of each level and solving (13) and (14) for the first section of the device, the active region gain of all three signals and their photon density are calculated as a function of time for the first section. Then, solving the fifteen ODE equations by ODE45 command of MATLAB software, the occupation probabilities of each level for the second section are estimated as a function of time. After that, the amplitude of all signals in the second section as a function of time is calculated by using the gain of the first section and the amplitude of input signals. The obtained values at the last time will be the optical amplitude in the second section. This process is repeated to calculate the new amplitude for spatial evaluation.

By calculating the amplitude of the conjugate signal in the last section of QD-SOA, from (15), the FWM efficiency is calculated. The detuning

frequency is the difference frequency between the pump and the probe, as follows:

$$f = c.\left(\delta_{\text{pump}} - \delta_{probe}\right) \tag{21}$$
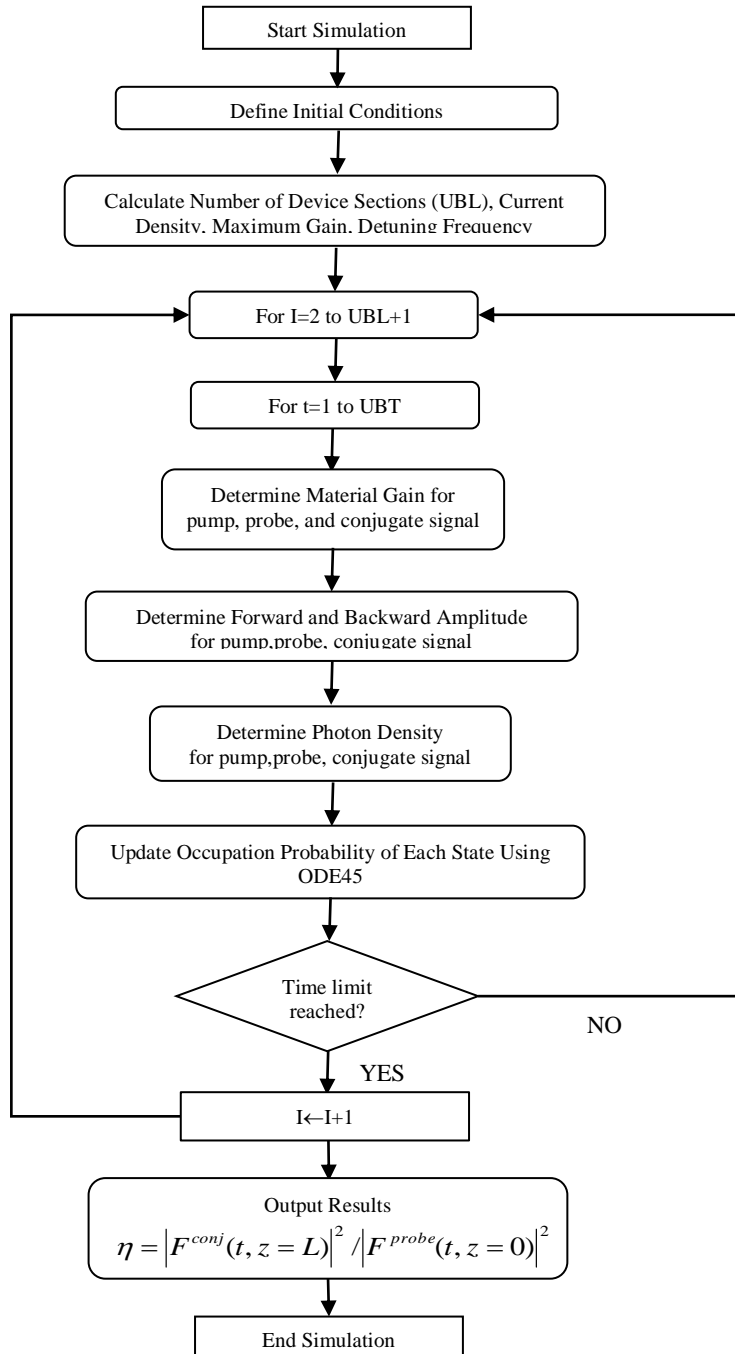
Fig. 3. The algorithm for calculating FWM efficiency of QD-SOA.

According to (21), FWM is calculated for different frequencies by changing δ_{probe}. The values of the physical quantities used in this modeling are presented in Table III.
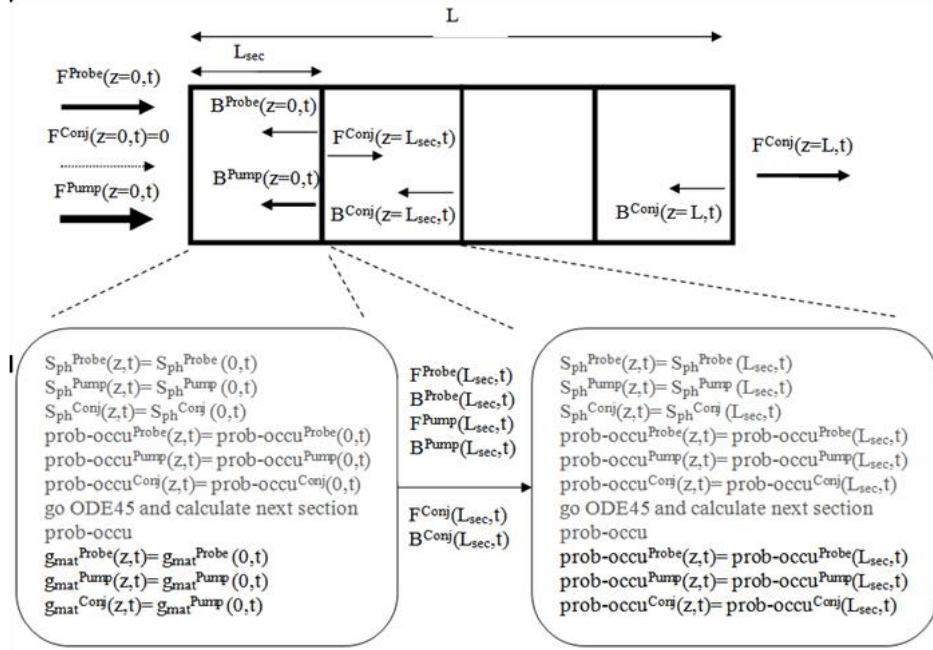
Fig. 4. The SILCE Technique for modeling FWM efficiency.

5. RESULTS OF FWM MODELING

In this paper, it has been carried out numerical modeling of QD-SOA for calculating the FWM efficiency. QD-SOA modeling was performed with MATLAB software.

Using a Core 2 Duo laptop with 2 GB of memory, the runtime is less than 5 minutes. This time seems to be less than what was mentioned in [12].

In Fig. 5, the occupation probabilities of each level in the last section as a function of levels number are shown. The occupation probabilities from 0 to 1 indicate the validity of the results. As shown, occupation probabilities for CB are very large while the occupation probability for VB is small for similar levels. The small value of similar levels in VB compared with CB is mainly due to fast escape in VB. This is due to the fact that the hole states are closely spaced (30 meV) i.e. the separation energy between levels in VB is small in comparison CB. Furthermore, the highest filling was related to GS, ES1, and ES2 of the CB and also ES1 of the VB, respectively.

TABLE II
PHYSICAL PARAMETERS USED IN MODELING

Symbol	Parameter
α_0	5.6×10^{-17} cm^{-1}
α_H	1
α_l	2.3 cm^{-1}
N_Q	2.5×10^{17} cm^{-3}
Σ	30 meV
$\tau_{i+1,i}{}^n$	8 ps
$\tau_{i+1,i}{}^p$	1 ps
$\tau_{i,i+1}{}^n$	1.5 ps
τ_{iR}	0.2 ns
$\hbar\omega_0{}^{max}$	0.95ev
$\hbar\omega_1{}^{max}$	1.04ev
$\hbar\omega_2{}^{max}$	1.14ev
g_0	14 cm^{-1}
g_1	20 cm^{-1}
g_2	10 cm^{-1}
I	288 mA
K	60
W	1μm
L	2.5 cm
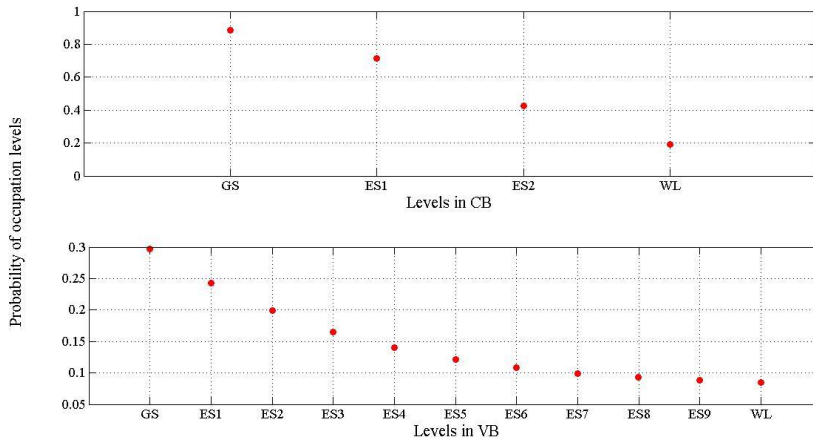
Fig. 5. Occupation probabilities of each level in the last section for CB and VB, separately.

The FWM efficiency as a function of detuning frequency shows in Fig. 6. As the frequency increases, the FWM efficiency decreases. In this case, the carriers are reduced in WL and therefore the efficiency is expected to decrease. Figure (6) has a good agreement with other simulated data and even experimental data [18-19] and [2]. In our model, the highest efficiency of FWM occurred at zero detuning frequency like recent paper [2] and [6]. The error rate of our models is less than 5% in comparison with [10]. When the separation energy between the energy levels is low, the escape of the carrier from the GS increases and then the occupation probabilities in the ES and WL increase. This increase causes the occupation probabilities in GS to decrease, i.e the FWM decreases [10].

Therefore, QD-SOA exhibits a higher efficiency due to the higher quantization of states in comparison with other semiconductors [10].
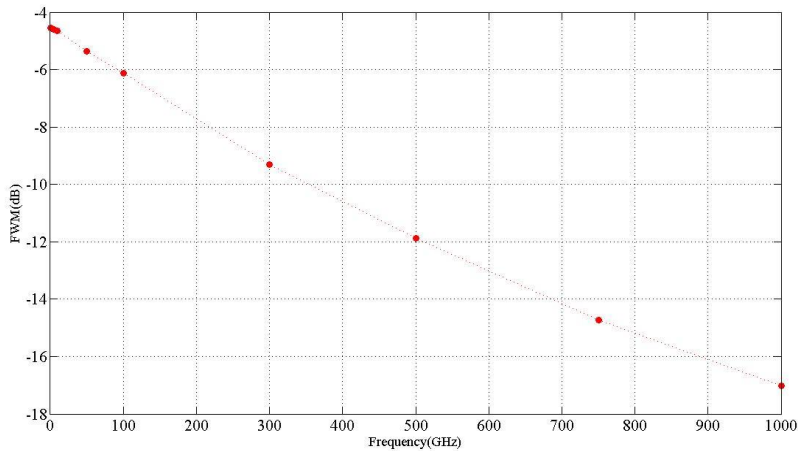
Fig. 6. FWM efficiency of different values of frequency.

The gain of pump and probe as a function of detuning frequency is shown in Fig. 7. As can be seen, the gain of the probe increases with increasing detuning frequency and then reaches the gain of the pump with a negative slope at a certain frequency, while the gain of the pump remains almost constant.

This characteristic has a good agreement with [10]. For example, at the detuning frequency of 1000 GHz, the error rate for the FWM efficiency in our model is less than 0.5% in comparison with [10].
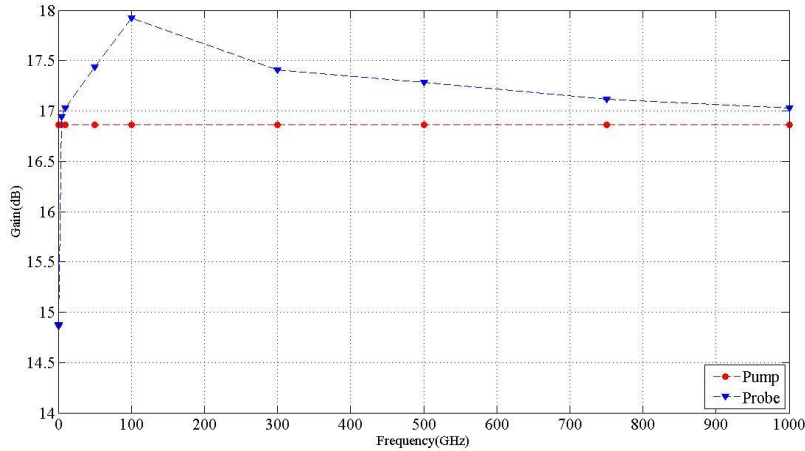
Fig. 7. Optical gain of the pump and probe as a function of detuning frequency.

In Figure (8), the FWM efficiency as a function of detuning frequency under the different lengths of the device is shown. As can be seen, the efficiency increases by the increasing length of the amplifier. It is expected the beating between pomp and probe increases, when length of amplifier increases and consequently, the FWM could be more significant. An acceptable efficiency from L= 2 to L=3 cm is provided, while characteristic is not flat for the length is less than 1.5 cm. This roughness is more clearly visible for L=1.5 cm. Since FWM is only obtained in the nonlinear regime of the device, this roughness indicates that the QD-SOA is out of the nonlinear regime named highly nonlinearly range [2].

In highly nonlinear range, the optical signal is strong enough to completely bleach the optical transition and the gain medium becomes transparent. This range is characterized not only by the transparency of the gain medium, but also by the appearance of nonlinear Rabi oscillations of the charge-carrier occupation densities in the quantum dots [2]. However, the efficiency curves for length less than 1.5 cm become slightly deformed in highly nonlinear regime.
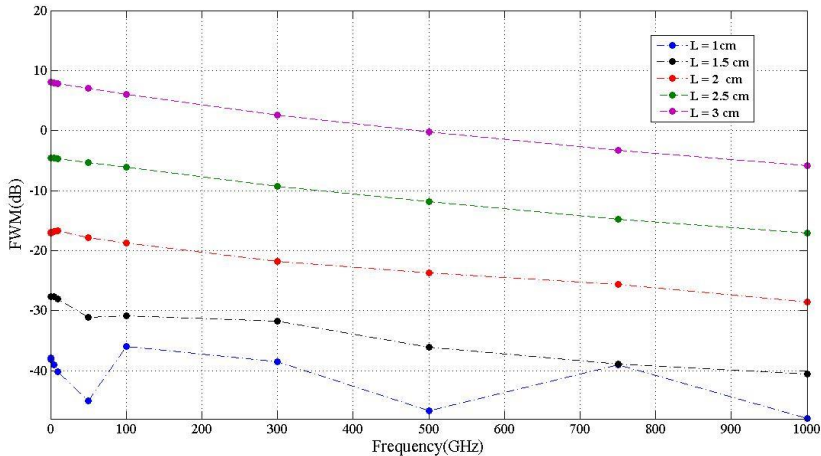
Fig. 8. FWM efficiency as a function of detuning frequency for different lengths.

6. CONCLUSION

In this paper, a simple, fast, and accurate model for four-wave mixing (FWM) efficiency in the QD-SOAs was proposed. In this model, the efficiency of FWM in the QD-SOA is accurately evaluated using the rate equations and the transfer matrix based on the pump/probe measurement technique. In order to solve these highly coupled equations numerically, we introduced a novel algorithm using the SLICE Technique. The modeling results show a short runtime and remarkable accuracy compared with similar reported models. Therefore, the proposed model and the presented algorithm for solving equations are suitable for many applications such as computer-aided-design of QD-SOAs as the FWM wavelength converter.

REFERENCES

[1] V. Sasikala et al. *Effects of Cross-phase Modulation and Four-Wave Mixing in DWDM Optical Systems Using RZ and NRZ Signal*. Optical And Microwave Technologies. Springer. (2018).

[2] M. Zajnulina et al. *Four-Wave Mixing in Quantum-Dot Semiconductor Optical Amplifiers: A Detailed Analysis of the Nonlinear Effects*. IEEE J. Quantum Electron. 23(6) (2017-Dec) 1-12.

[3] A. Nosratpour et al. *Numerical analysis of four wave mixing in photonic crystal semiconductor optical amplifier*.Elsevier J.Optics Communications. 433(2019-Feb) 104-110.

[4] A. H. Flayyih et al. *Integral gain in quantum dot semiconductor optical amplifiers.* Superlattices and Microstructures. 62 (2013) 81-87.

[5] G. Contestabile et al. *Four wave mixing in quantum dot semiconductor optical* amplifiers. IEEE Journal of Quantum Electronics. 50(5) (2014 – Mar) 379-89.

[6] A. H. Flayyih et al. *Theory of four-wave mixing in quantum dot semiconductor optical amplifiers*. Journal of Physics D: Applied Physics. 46(44) (2013-Oct) 445102.

[7] A. H. Flayyih. *Theory of pulse propagation and four-wave mixing in a quantum dot semiconductor optical amplifier*. Current Applied Physics. 14(1) (2014-Jul) 946-53.

[8] A .H. Flayyih et al. *Four-Wave Mixing in Quantum Dot SOAs: Theory of carrier heating*. ELSEVIER Journal of Physics. 7 (2017-Jan) 1339-1345.

[9] B.Lingnau et al. *Rabi-oscillation-enhanced frequency conversion in quantum-dot semiconductor optical amplifiers*. Springer Journal oF Optical and Quantum Electronics. 50(2) (2018-Feb).

[10] O. Qasaimeh. *Theory of Four-Wave Mixing Wavelength Conversion in Quantum Dot Semiconductor Optical Amplifiers*. IEEE Photonics Technology Letters. 16(4) (2004-Apr) 993-995.

[11] F. Hakimian et al. *A Proposal for a New Method of Modeling of the Quantum Dot Semiconductor Optical Amplifiers*. Journal of Optoelectronical Nanostructures. 4(3) (2019-Aug) 1-16.

[12] S.M.Izadyar et al. *Quantum dot semiconductor optical amplifier: investigation of amplified spontaneous emission and noise figure in the presence of second excited state*. Springer Journal oF Optical and Quantum Electronics. 50(1)(2018-Jan)5.

[13] H.Taleb et al. *Quantum-Dot Semiconductor Optical Amplifiers: State Space Model versus Rate Equation Model*. Advances in OptoElectronics. 2013(2013).

[14] O. Qasaimeh. *Linewidth enhancement factor of quantum dot lasers*. Optical and Quantum Electronics. 37(5) (2005-Apr) 495–507

[15] F. Hakimian et al.*Optimization of a quantum-dot semiconductor optical amplifier (QD-SOA) design using the genetic algorithm*. Optical and Quantum Electronics. 52(1) (2020-Jan) 1-19.

[16] O.Qasaimeh. *All-optical multistability using cross-gain modulation in quantum-dot distributed feedback semiconductor optical amplifier*. Optical and Quantum Electronics. 50(2)(2018-Feb)54.

[17] O. Qasaimeh. *Efficiency of four-wave mixing of doped closely spaced energy states quantum dash semiconductor optical amplifiers*. Optical Engineering. 50(9) (2011-sep).

[18] A. H. Flayyih et al. *Four-Wave Mixing Conversion in QD SOA: reservoir effects.* JOURNAL OF THI-QAR SCIENCE. 6(3) (2017) 30-34.

[19] T. Akiyama et al. *Symmetric highly efficient (/spl sim/0 dB) wavelength conversion based on four-wave mixing in quantum dot optical amplifiers*. IEEE Photonics Technology Letters. 14(8)(2002-Nov)1139-1141.